© 2014. Published by The Company of Biologists Ltd | Development (2014) 141, 3605-3611 doi:10.1242/dev.114546

RESEARCH ARTICLE

A dynamic analysis of muscle fusion in the chick embryo

Daniel Sieiro-Mosti, Marie De La Celle, Manuel Pelé and Christophe Marcelle*

ABSTRACT

Skeletal muscle development, growth and regeneration depend upon the ability of muscle cells to fuse into multinucleated fibers. Surprisingly little is known about the cellular events that underlie fusion during amniote development. Here, we have developed novel molecular tools to characterize muscle cell fusion during chick embryo development. We show that all cell populations arising from somites fuse, but each with unique characteristics. Fusion in the trunk is slow and independent of fiber length. By contrast, the addition of nuclei in limb muscles is three times more rapid than in trunk and is tightly associated with fiber growth. A complex interaction takes place in the trunk, where primary myotome cells from the medial somite border rarely fuse to one another, but readily do so with anterior and posterior border cells. Conversely, resident muscle progenitors actively fuse with one another, but poorly with the primary myotome. In summary, this study unveils an unexpected variety of fusion behaviors in distinct embryonic domains that is likely to reflect a tight molecular control of muscle fusion in vertebrates.

KEY WORDS: Electroporation, Chick embryo, Limb, Muscle fusion, Myotome

INTRODUCTION

During embryogenesis and early adult life, skeletal muscle fibers grow through the addition of new myonuclei, which are supplied by resident muscle progenitors during embryogenesis and by satellite cells after birth. Fusion can be extensive: the longest muscle fibers of the human thigh contain tens of thousands of nuclei. Although the number of muscle fibers does not change after birth, the number of nuclei per fiber continues to increase until puberty (Shavlakadze and Grounds, 2006; White et al., 2010). Myoblast fusion is not only crucial for fiber growth, but also for muscle repair in adults after injury or in pathological conditions such as myopathies (Rochlin et al., 2010; Simionescu and Pavlath, 2011; White et al., 2010).

Very little is known about the dynamics of muscle fusion in mammalian development. This is due to the poor accessibility of mouse to observation, the high complexity of the muscle tissue and the lack of specific tools to characterize myoblast fusion in this organism. By contrast, the fruit fly *Drosophila melanogaster* has been a major source of knowledge on muscle fusion, both at the cellular and molecular levels. In fly, two types of myoblasts contribute to muscle formation: muscle founder cells (FCs) and fusion-competent myoblasts (FCMs); FCs function as 'attractants' for the surrounding FCMs. Muscle fusion in the *Drosophila* embryo occurs over a 5.5 h period during late embryogenesis and results in the formation of multinucleated myotubes that can contain as few as two to as many as 24 nuclei per muscle fiber (Bate, 1990). Electron microscopy studies in the fly revealed that muscle fusion follows an ordered set of cellular events: recognition, adhesion, alignment, and membrane union resulting in the formation of a single multinucleated cell. Significantly, this process bears much resemblance at the cellular and ultrastructural levels with observations made *in vitro* using various murine and human muscle cell lines (Doberstein et al., 1997; Knudsen and Horwitz, 1977; Rash and Fambrough, 1973; Wakelam, 1985), suggesting that similar basic mechanisms underlie muscle fusion in vertebrates and invertebrates. In support of this hypothesis, recent studies on the molecular mechanisms regulating fusion in vertebrates (fish and rodents) have shown conservation with *Drosophila* (Horsley et al., 2001, 2003; Moore et al., 2007; Richardson et al., 2008; Srinivas et al., 2007). How much of the cellular and molecular strategies observed in the fly are conserved in vertebrates is unknown.

Amniote muscle derives from two main muscle progenitor populations that emerge sequentially in early embryos: the myocytes of the primary myotome and the resident muscle progenitors. Myocytes are generated in a first stage of myogenesis by cells arising from the four epithelial borders of the dorsal compartment of somites termed the dermomyotome. They organize into a primitive skeletal muscle called the 'primary' myotome (Denetclaw and Ordahl, 2000; Gros et al., 2004; Kahane et al., 2002). Resident muscle progenitors appear during a second stage of muscle morphogenesis. They originate from the central portion of the dermomyotome and invade the primary myotome after an epithelial-to-mesenchyme transition (EMT). In the trunk of the chick embryo, the EMT is observed at 4 days of development, whereas in the trunk of mouse embryos it is observed at embryonic day 10.5 (E10.5). Resident progenitors massively contribute to the formation of all muscles of the body and they later generate the adult muscle stem cells, termed satellite cells (Ben-Yair and Kalcheim, 2005; Delfini et al., 2009; Gros et al., 2005; Kassar-Duchossoy et al., 2005; Manceau et al., 2008; Relaix et al., 2005). In limbs, muscles derive from one wave of progenitors that migrate from the lateral portion of somites into the lateral plate-derived limb mesenchyme, where they differentiate (Chevallier et al., 1976; Christ et al., 1974; Schienda et al., 2006). Whether different muscle progenitor populations fuse and at what rate is unknown.

The amenability of the chick embryo to observation and imaging, combined with the electroporation technique that allows lineage and cell fate analyses, provide a unique environment to characterize the cellular and molecular mechanisms regulating fusion in amniotes. In this study we have analyzed the routes that myocytes and resident muscle progenitors follow to become multinucleated, from the time of the first fusion events to the first days of muscle development. We developed genome-integrated vectors and double electroporation protocols that allow the labeling of cells within the same or distinct populations with different fluorescent proteins. Using these techniques, we determined that the rate and partners of fusion, as well as nuclei occupancy, vary significantly in distinct embryonic domains.

EMBL Australia; Australian Regenerative Medicine Institute (ARMI), Monash University, Building 75, Clayton, VIC 3800, Australia.

*Author for correspondence (christophe.marcelle@monash.edu)

Received 19 June 2014; Accepted 30 July 2014

Development (2014) 141, 3605-3611 doi:10.1242/dev.114546

RESULTS

Varying rate and mode of fusion during trunk and limb muscle morphogenesis

We determined whether the muscle populations that have been identified in chick embryos undergo fusion and at what rate.

Construction of a vector to evaluate fusion

Muscle fibers within growing muscle masses (in limb or somites) are tightly intertwined and it is practically impossible to distinguish single fibers from end-to-end and count nuclei with classic immunostaining techniques, even with confocal imaging. By contrast, the electroporation technique results in the mosaic expression of transgenes and we hypothesized that this property, together with the use of appropriate fluorescent reporters and confocal imaging, would allow the identification of individual fibers and the evaluation of the number of nuclei per fiber within this complex tissue. We constructed a vector that contains a nuclear RFP variant, NLSmCherry and a membrane EGFP (see Materials and Methods). Cis-sequences from the Tol2 transposable element were inserted on both sides of the fluorochromes, allowing their permanent integration into the genome of host cells. This eliminates the gradual dilution of the transfected episomal plasmid with cell divisions.

Fusion of myocytes derived from the DML

We electroporated the medial portion of newly formed epithelial somites in the interlimb region as previously described (Scaal et al., 2004). This leads to the specific labeling of the medial border of the dermomyotome (the DML; Fig. 1A), from which emerge the first myocytes of the primary myotome (Gros et al., 2004; Ordahl et al., 2001). We counted the number of nuclei in electroporated (GFP^+/RFP^+) myosin heavy chain (MyHC)-positive cells at successive developmental stages. Twenty-four hours after electroporation (at E3.5), nearly all electroporated myocytes contained only one nucleus. A small proportion of them contained two or three nuclei (Fig. 1B,C,L; mean nuclei number at E3.5, 1.1; see supplementary material Table S1). The number of nuclei per myofiber increased slightly, but significantly, at the next time point (Fig. 1D,E,L; mean nuclei number, 1.3; $P<0.001$). The rate of fusion increased strongly thereafter, and at E5.5 we observed myocytes containing up to seven nuclei (Fig. 1F,G,L; mean nuclei number, 2.7; $P<0.0001$). The mean fusion rate, expressed as the number of hours needed to add one nucleus to the entire population of electroporated myocytes, reached 16.4 h at the peak of fusion, occurring between E4.5 and E5.5 (see Fig. 3A). However, individual myocytes may fuse much more quickly, since some contained up to seven nuclei at E5.5 (whereas one day earlier, most were mononucleated), suggesting a maximal rate of fusion in individual fibers of one nucleus added every 4 h (about six nuclei per 24 h) between E4.5 and E5.5.

We observed that all myocytes, regardless of the number of nuclei, spanned the entire width of somites, indicating that nuclei number is independent of fiber length. To confirm this, we tested the correlation between fiber length and nuclei number and found that, during the time of our experiments, the two variables were not significantly linked (Fig. 3D).

Fusion of resident muscle progenitors

We then electroporated the dorsal portion of newly formed somites in the interlimb region as previously described (Gros et al., 2005). This leads to the specific labeling of the population of resident progenitors in the central dermomyotome that enter the primary myotome 36 h after somite formation (Gros et al., 2005). At E4.5,

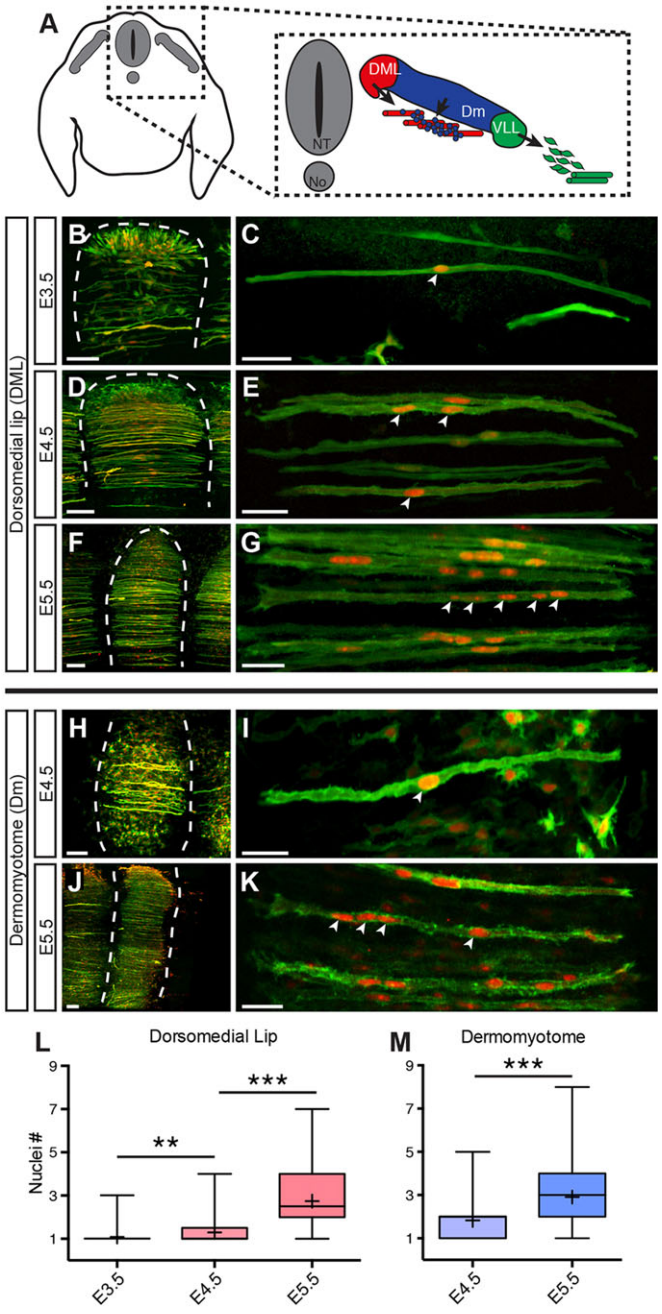

Fig. 1. Analysis of fusion in the trunk. (A) Diagram showing a transverse view of the E5 chick embryo. At the interlimb level, the medial border of the dermomyotome (DML), the lateral (VLL), as well as the anterior and posterior borders (not shown) contribute to the formation of the primary myotome, which is composed of myocytes (red), while the central dermomyotome (Dm) generates resident muscle progenitors (blue). At the limb level, muscle progenitors from the VLL (green) migrate into the limb mesenchyme, where they differentiate. NT, neural tube; No, notochord (B-G) Cells from the DML were electroporated at E2.5 and nuclei number per fiber was counted at E3.5 (B,C), E4.5 (D,E) and E5.5 (F,G). (H-K) Cells from the central dermomyotome were electroporated at E2.5 and analyzed at E4.5 (H,I) and E5.5 (J,K). All images are whole-mount confocal stacks of fixed embryos, immunostained for EGFP (green) and RFP (red). Dashed lines delineate somites at the end of experiments. Arrowheads (C,E,G,I,K) indicate cell nuclei within selected fibers. (L,M) Quantification of nuclei number per fiber at the time points in B-G (L) and H-K (M). Whiskers indicate minimal and maximal values; the bottom and top of the box indicate the first and third quartile; the horizontal line indicates the median; and '+' indicates the mean for each set of values. $^{**}P<0.001$; $^{***}P<0.0001$. Scale bars: 100 µm in B,D,F,H,J; 50 µm in C,E,G,I,K.

Development (2014) 141, 3605-3611 doi:10.1242/dev.114546

48 h after somite formation, 90% of the cells derived from the central dermomyotome are proliferating Pax7-positive resident progenitors (Gros et al., 2005), which display a mesenchyme-like morphology. However, a small proportion of electroporated cells spanned the entire width of somites. These were morphologically similar to the myocytes derived from the DML, expressed the terminal differentiation marker MyHC (not shown; Gros et al., 2005) and contained an average of 1.8 nuclei (Fig. 1H,I,M; supplementary material Table S1). At E5.5, the number of nuclei significantly increased and myofibers containing up to eight nuclei were observed (Fig. 1J,K,M; mean nuclei number, 2.9; $P<0.0001$). The mean rate of fusion of muscle progenitors from E4.5 to E5.5 is therefore one nucleus every 22 h, with a maximal rate very close to that observed in the DML-derived population (one nucleus per 4.5 h; Fig. 3B).

We also observed that resident progenitors in the trunk somites first elongate until they reach the somite borders, and then accumulate nuclei with no significant fiber growth. Thus, similar to DML-derived myocytes, during the time frame of our analysis there is no significant link between fiber length and nuclei number in myocytes derived from the population of trunk-resident progenitors (Fig. 3D).

Fusion of limb muscle progenitors

In order to study muscle fusion in the limb, we electroporated the lateral portion of newly formed somites in the forelimb region (somites 16-21). This leads to the specific labeling of the lateral border of the dermomyotome (the VLL) from which all limb muscle progenitors emanate (Fig. 1A). We analyzed electroporated embryos at E4, E4.5, E5, E5.5 and E6, focusing our study on the dorsal muscle masses of the limb. We counted the number of nuclei in MyHC/GFP-positive cells. At E4, very little MyHC staining was observed (Fig. 2A). Of those cells, nearly all were mononucleated (89%; Fig. 2A-C,P; mean nuclei number, 1.1; supplementary material Table S1). Between E4 and E4.5, the number of nuclei did not change significantly (Fig. 2D-F,P; mean nuclei number, 1.2). From E4.5 onward (Fig. 2G-O), the number of nuclei per MyHC^{+} myofiber dramatically increased, and fibers with up to 16 nuclei were observed at E5.5 (arrowheads in Fig. 2L), which is only 1 day after the initiation of fusion at E4.5. The mean number of nuclei also sharply increased during this period, from 1.2 (E4.5) to 4.3 (E5) to 5.6 (E5.5) and finally 7.2 (E6) (Fig. 3C; supplementary material Table S1). The sharpest increase in the mean fusion rate was observed between E4.5 and E5.5, when one nucleus was added every 5 h. Again, in individual myogenic cells, this rate may be much faster, with a maximum rate of around one nucleus added every 1.5 h (15 nuclei added in 24 h). We did not quantify the fusion rate of the ventral muscle masses of the forelimb, but the overall fusion pattern was similar to that of the dorsal ventral mass (supplementary material Fig. S1).

In sharp contrast to the situation observed in the trunk, it was apparent that, as the embryos developed, limb muscle fibers

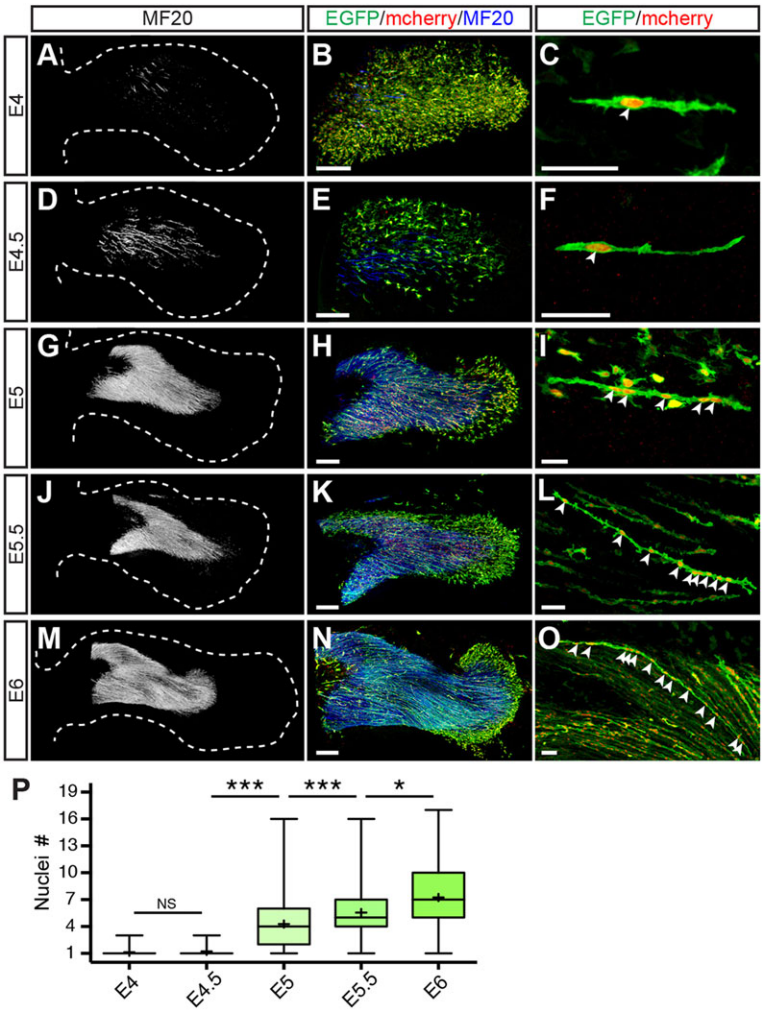

Fig. 2. Analysis of fusion in the dorsal muscle masses of chick forelimbs. (A-O) Cells from the VLL at forelimb level (somites 16-21) were electroporated at E2.5. The nuclei count per fiber was performed at E4 (A-C), E4.5 (D-F), E5 (G-I), E5.5 (J-L) and E6 (M-O). All images are whole-mount confocal stacks of fixed embryos. (A,D,G,J,M) Forelimbs (delineated by dashed lines) are immunostained for MyHC (white) to show the muscle masses; in all other images, blue is MyHC, green is EGFP and red is mCherry. Arrowheads (C,F,I,L,O) indicate cell nuclei within selected fibers. (P) Quantification of nuclei number per fiber at the time points in A-O (see Fig. 1 legend). *$P<0.05$; ***$P<0.0001$. Scale bars: 200 µm in B, E,H,K,N; 50 µm in C,F,I,L,O.

Development (2014) 141, 3605-3611 doi:10.1242/dev.114546

became longer and contained an increasing number of nuclei (Fig. 2C,F,I,L,O). To confirm this, we tested the correlation between fiber length and nuclei number and found that the addition of nuclei was very significantly linked to fiber growth, and each additional nucleus was accompanied by an increase in fiber length of ~40 µm (Fig. 3E).

A complex matchmaking underlies trunk muscle fusion

Since myocytes of the primary myotome and resident progenitors initiate fusion after E4, i.e. immediately after the EMT of the dermomyotome is initiated (Gros et al., 2005), we hypothesized that both populations might fuse to one another. To address this, we devised protocols that allow the labeling of cells within a population with different fluorescent proteins. If these populations fused, both fluorescent proteins would be observed within one multinucleated fiber.

Construction of vectors to label a single population with two fluorochromes

It was reported that the efficiency of electroporation may be cell cycle-dependent (Brunner et al., 2002; Goldstein et al., 1989). Epithelial cells in the chick DML cycle asynchronously, with an estimated cell cycle length of 9-11 h (Primmett et al., 1988; Venters et al., 2008). We hypothesized that by electroporating the DML with two plasmids coding for GFP or for mCherry (a variant of RFP) 5 h apart, we would transfect distinct populations of cells, if indeed electroporation were cell cycle dependent. We found that a reasonable percentage (41.4%) of epithelial cells in the DML expressed only one fluorochrome when electroporated 5 h apart with mCherry or GFP, although a majority expressed both (58.6%; Fig. 4A,C; supplementary material Table S2).

Since this technique was not suitable for our purpose, we designed a new set of vectors that, combined with double electroporation, would result in the exclusive expression of either cytoplasmic EGFP or mCherry, but not both (see Materials and Methods; supplementary material Fig. S2A-D). We verified the efficiency of this approach by electroporating the DML consecutively with the two sets of vectors. Ten hours later, mononucleated myocytes were examined for GFP or mCherry expression and only 3.4% expressed both fluorochromes (Fig. 4A,D; supplementary material Table S2). This number thus represents the 'leakiness' of the labeling system that we devised and it was used to modulate the percentage of fusion observed in the following experiments [mean percentage (adjusted) in supplementary material Table S2].

Primary myocytes and resident progenitor fusion

Using these plasmids, we first electroporated the DML. Three days later, we analyzed the color of bi-nucleated myocytes (i.e. resulting from one fusion event). We observed that 49.7% of bi-nucleated myocytes expressed GFP, while 42.2% were mCherry positive and 8.2% expressed both (Fig. 4A,E,F; supplementary material Table S2). This indicates that the vast majority of cells generated at the DML do not fuse with one another. The small increase in yellow cells is not significantly different to the control, although it might indicate that a small percentage of DML cells nevertheless fuse.

We then electroporated this combination of plasmids into the dorsal dermomyotome, from which resident progenitors arise. Three days later 36.7%, 30.2% and 33.1% of bi-nucleated myocytes were green, red and yellow, respectively (Fig. 4A,G,H; supplementary material Table S2). This is significantly different to the control values and indicates that resident progenitors readily fuse to one another.

Primary myocytes do not fuse to resident progenitors

Using the same combination of vectors as above, we labeled the DML with GFP and the dorsal dermomyotome with mCherry. Three days later, we analyzed bi-nucleated cells in regions of the myotome, where GFP^+ cells were adjacent to $mCherry^+$ cells. Surprisingly, we observed that 48%, 42.7% and 9.3% expressed GFP, mCherry and both, respectively (Fig. 4A,I,J; supplementary material Table S2). The proportion of yellow cells is not significantly different to the control, indicating that DML myocytes do not fuse to progenitors. The slight increase in fusion might, however, indicate that they marginally fuse. GFP^+ and $mCherry^+$ cells were mostly intimately intertwined (Fig. 4J), suggesting that the low numbers of bi-labeled cells observed are unlikely to be due to a lack of proximity of the analyzed cells. This puzzling result prompted us to identify the cells that fuse with the DML-derived cells.

The anterior and posterior borders of the dermomyotome also generate myocytes, which intermingle with DML-derived cells (Gros et al., 2004). We determined whether these two cell populations fuse to DML-derived cells. We labeled the DML with GFP and either the anterior or the posterior border with mCherry. Importantly, the exclusive labeling vector system we used ensures that cells at the medio-anterior or medio-posterior corner of the dermomyotome are labeled with only one fluorescent protein in the event that they are electroporated twice in the procedure. When the

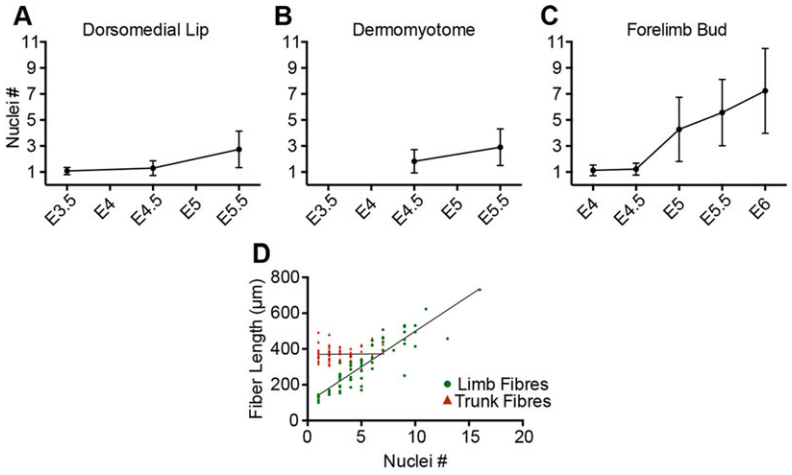

Fig. 3. Fusion rates of muscle cells and ratio of fiber length to nuclei number for different regions. (A-C) Fusion rates of muscle cells derived from the DML (A) or from the central dermomyotome (B) and in the forelimb muscle masses (C) were determined in chick embryos electroporated at E2.5 and tested at the indicated incubation times. Each point represents the mean nuclei per fiber in all electroporated cells; bars represent s.d. (D) Ratio of fiber length to nuclei number in the trunk (red) and limb (green). The best-fitting lines for the observed data indicate that in the trunk (D) there is no significant correlation between fiber length and nuclei number [Pearson's product-moment correlation $r(77)=0.19$, $P=0.09$]. By contrast, there is a strong correlation between fiber length and nuclei number in the limb [$r(58)=0.89$, $P<2.2^{-16}$; $y=39.7x+102.1$ (equation of the line of best fit)].

Development (2014) 141, 3605-3611 doi:10.1242/dev.114546

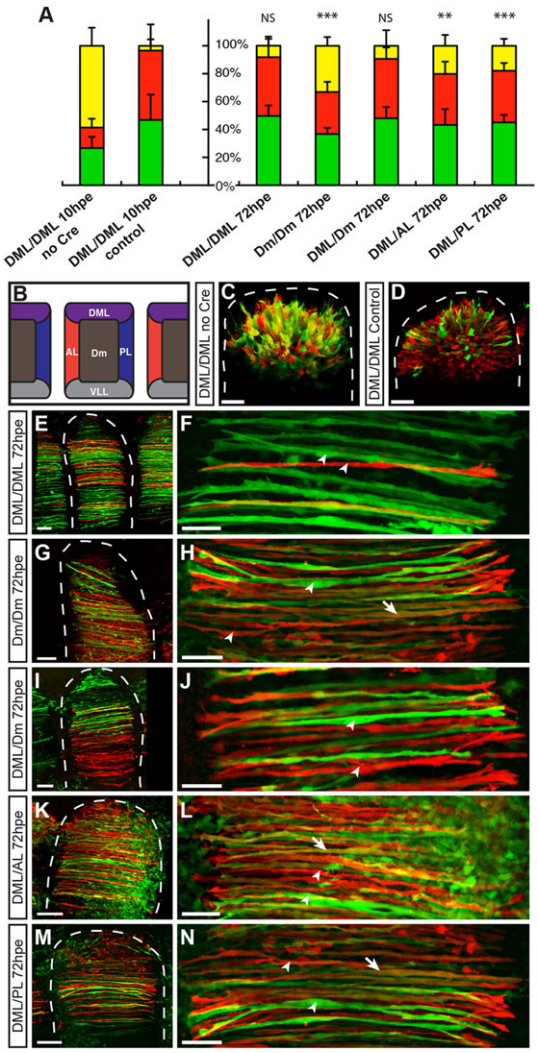

Fig. 4. Primary myotome cells do not fuse to resident muscle progenitors. (A) The percentage of fusion within cell populations electroporated with EGFP and mCherry at E2.5 and tested 10 (C,D) or 72 (E-N) hours post electroporation (hpe). Error bars indicate s.d. ***P*<0.001; ****P*<0.0001; NS, not significant. (B) Diagram showing a dorsal view of trunk somites in an E2.5 chick embryo. The regions of the somite that were electroporated in C-N are indicated: central dermomyotome (Dm) and medial (DML), lateral (VLL), anterior (AL) and posterior (PL) borders. (C,D) DML cells were double electroporated with EGFP-expressing and mCherry-expressing vectors 4-5 h apart (C), or with Cre-mediated EGFP-excluding and mCherry-excluding vectors (see Material and Methods), the latter resulting in a minor proportion of yellow cells (containing both fluorophores) 10 h post electroporation, i.e. before fusion is initiated (A, second bar). (E-N) Bi-nucleated fibers expressing EGFP (green), mCherry (red) or both (yellow) were counted 72 h post electroporation (see A). All images are whole-mount confocal stacks of fixed embryos immunostained for EGFP and mCherry. Arrowheads (F,H,J,L,N) indicate selected single-labeled fibers; arrows (H,L,N) indicate selected double-labeled fibers. Dashed lines delineate somites at the end of experiments. Scale bars: 100 µm in E,G,I, K,M; 50 µm in C,D,F,H,J,L,N.

DML was electroporated together with the anterior border of the dermomyotome, we observed after 72 h of incubation that 43.3%, 36.6% and 20.1% expressed GFP, mCherry and both, respectively. Likewise, when the DML was electroporated together with the posterior border, we observed after 72 h of incubation that 45.1%, 37.1% and 17.8% expressed GFP, mCherry and both, respectively. In each case, the percentage of yellow bi-nucleated myocytes was significantly higher than in the controls. These data indicate that DML cells fuse equally to cells emanating from the anterior or posterior borders of the dermomyotome.

DISCUSSION

Altogether, our findings demonstrate that electroporation and confocal imaging allow a precise quantification of nuclei number in muscle fibers *in vivo* despite the increasing complexity of muscle masses as the embryo grows. Since electroporation targets seemingly random cells within somites, their progeny are evenly distributed within muscle masses, such that this allows a representative sampling of the entire population with no positional bias. Although this might not be crucial in somites, where fibers containing one or more nuclei are evenly distributed as fusion proceeds, it is important in limbs, where fibers containing the most nuclei are preferentially localized in the center of the muscle masses. Our analysis showed that the three muscle cell populations that we tested fuse. Although this was expected for resident progenitors in the trunk and the limb, which constitute the main reservoir of all muscles, it was however unknown whether myocytes of the primary myotome fuse as well. We had previously shown that myocytes become progressively diluted by fibers derived from the resident progenitor population, and that they constitute a negligible portion of the fetal muscle masses (Gros et al., 2005). Our current data indicate that, despite this, the primary myocytes generate bona fide multinucleated fibers that participate to the formation of embryonic muscles.

Our results show that, during early embryogenesis, muscle fusion in limb and trunk display distinct features. In trunk muscles, nuclei fused while the length of myofibers hardly changed. Since the diameter of myofibers was not significantly modified during the time frame of the experiment (Fig. 1), this implies that the volume of cytoplasm supported by each nucleus (the nuclear domain) decreased during that period. This differs from the widely accepted ‘karyoplasmic ratio hypothesis’, which postulates that cell and nuclear volumes are linked (Bruusgaard et al., 2003; Cavalier-Smith, 1978). By contrast, each additional nucleus in limb myofibers was accompanied by an increase in fiber length, indicating that, in limb muscles, the nuclear domain was constant during the period of the experiment.

A second feature that distinguishes trunk and limb muscle fusion is that the fusion rate is nearly identical in both populations of trunk progenitors, regardless of their origin, fate or cellular characteristics (e.g. resident progenitors are proliferative, display stem cell-like attributes, contribute to a variety of hypaxial and epaxial muscles; DML-derived primary myocytes readily differentiate, are postmitotic and contribute exclusively to epaxial muscle masses). By contrast, muscle fusion in early limb differentiation was much faster than in the trunk, with a maximal rate of one nucleus added every 1.5 h. This suggests that, at least during the time frame of this study, the fusion rate is defined at the level of the body region. The maximal rate of muscle fusion that we observed in the limb (1.5 nuclei/h) is remarkably similar to that observed in isolated fibers from mouse extensor digitorum longus muscle during a period of intense growth in the first two postnatal weeks (1.8 nuclei/h; White et al., 2010), and this number might in fact correspond to the maximal rate of muscle fusion in amniotes.

Following the characterization of chick myoblast fusion, we had aimed to determine whether some of the stereotyped patterns of fusion uncovered in flies are conserved in amniotes. In particular, it was interesting to determine whether myoblasts of the primary myotome act similarly to *Drosophila* myoblasts, the defining

Development (2014) 141, 3605-3611 doi:10.1242/dev.114546

characteristic of which is their complete inability to fuse with their own type. Our data suggest that this is not the case in chick, since resident progenitors mainly fuse with each other, and cells of the primary myotome fuse among themselves, but following a complex interaction with the neighboring lips. It is however possible that, within each population that fuses, cells with founder-like and fusion competence-like characteristics co-exist.

It was previously shown that the morphogenetic processes leading to the emergence of the resident progenitor and the primary myotome cell populations are clearly distinct (Gros et al., 2004, 2005). The gene networks regulating their differentiation are also different, since primary myotome formation is independent of Pax3 and Pax7 function, whereas resident muscle progenitors are absent when Pax3 and Pax7 function is abrogated (Kassar-Duchossoy et al., 2005; Relaix et al., 2005). That they do not readily fuse to each other further distinguishes these two cell populations.

In conclusion, this study of muscle fusion in the chicken embryo has uncovered the dynamics that orchestrate early myoblast fusion in amniotes. It will serve as a conceptual framework upon which future studies can rely to uncover the molecular mechanisms regulating this fascinating process. How this is controlled at the molecular level is unknown, but it is likely that a tightly knit network of inhibitors and activators of muscle fusion underlies the complex cell behaviors that we have revealed in this study.

MATERIALS AND METHODS

In ovo electroporation

Fertilized chick eggs were incubated at 38°C in a humidified incubator. Embryos were staged according to days of incubation. Newly formed somites were electroporated as previously described (Gros et al., 2004, 2005; Rios et al., 2011). Briefly, interlimb somites were electroporated so that only the borders of the dermomyotome (medial, lateral, anterior and posterior) or the central region of the dermomyotome would be electroporated. To follow limb muscle progenitor fusion, the lateral border of somites in the wing region (somites 16-21) was electroporated. One day after electroporation, the embryos were examined under UV light and those that were not adequately electroporated were discarded. We and others have shown previously that the electroporation process itself is harmless to the normal differentiation of electroporated cells. Electroporated embryos were analyzed after the indicated incubation times by fixing and processing for whole-mount immunostaining against GFP and RFP.

Plasmids used for electroporation

Construction of vectors to count the number of nuclei per fiber

To easily count the number of nuclei of electroporated cells, we constructed a plasmid (Tol2-CAGGS-NLSmCherry-IRES-mEGFP) that leads to the co-expression of membrane GFP and nuclear mCherry fluorochromes under the control of the ubiquitous CAGGS promoter (supplementary material Fig. S2A). This plasmid was constructed by a triple Gateway reaction using the following donor plasmids: (1) p5E-CAGGS, containing the strong, ubiquitous CAGGS promoter (CMV/chick β-actin promoter/enhancer; kindly provided by Dr James Godwin, ARMI, Australia); (2) NLSmCherry, containing the monomeric form of Cherry linked to a nuclear localization signal; and (3) IRES-mEGFP, containing EGFP with a C-terminal fusion of 21 amino acids of human Harvey Ras (HRAS) that encodes a prenylation signal that directs the GFP protein to the membrane. The destination plasmid was pDEST-Tol2pA2 (kindly provided by Dr Thomas Hall, ARMI, Australia). Tol2 integration sites at both ends of the constructs allow long-term integration into the genome of transfected cells in the presence of exogenously provided transposase protein.

Staining with DAPI and immunostaining for RFP showed that the nuclear mCherry marker was present in all nuclei within fluorescent multinucleated fibers. Since only a portion of cells within the muscle progenitor population are electroporated, this indicates that the nuclear mCherry marker is readily transferred to all nuclei within multi-nucleated fibers, regardless of whether they originated from electroporated cells. The number of nuclei in fibers at specific developmental stages was also calculated as follows: mean=$\Sigma x/n$, i.e. the sum of the number of nuclei in all fibers analyzed at that stage (x) divided by the number of fibers (n).

Vectors to determine whether progenitors within cell subpopulations fuse

To determine whether cells from the same somitic population can fuse to one another, we constructed three plasmids that were designed for two sequential electroporations 3-4 h apart.

In the first electroporation, two plasmids were co-electroporated (see supplementary material Fig. S2B). One contains (cytoplasmic) EGFP driven by the CAGGS promoter. However, the GFP is silent, due to a loxP-flanked (floxed) polyadenylation (polyA) site upstream of its initiation methionine. The second plasmid has a floxed *Cre* downstream of the CAGGS promoter. When the two plasmids are present in the same cell, the Cre removes the polyA site, GFP is translated and the cell is green under UV light. The Cre protein also excises itself, such that Cre protein is active only during a short period of time. If the two plasmids are not present in the same cell, GFP is silent.

Three to four hours later, a plasmid containing a floxed mCherry (i.e. a cytoplasmic monomeric Cherry variant of RFP) driven by CAGGS is electroporated into the same cell population (supplementary material Fig. S2C). Cells transfected with only this construct are red. If a cell already contains the plasmids electroporated in the first round (or the Cre plasmid only), the Cre inactivates the mCherry. In each round of electroporation, an additional plasmid coding for the transposase is added to allow Tol2-mediated genomic integration. We verified the efficiency of this approach and found that only 3.4% of (mononucleated) cells sequentially electroporated with these plasmids express both fluorochromes. This number thus represents the 'leakiness' of the labeling system that we devised. To estimate the true percentage of fusion, we therefore subtracted 3.4 from the percentage of GFP^+/RFP^+ and added half of this (i.e. 1.7) to each of the percentages of GFP^+ and RFP^+ that we obtained (these are referred to as 'adjusted' percentages of fusion; supplementary material Table S2).

Immunohistochemistry and confocal analysis

Embryos of the desired stages were dissected in PBS and fixed in 4% formaldehyde for 1 h.

For immunohistochemistry on whole-mount embryos, the following antibodies were used: chicken polyclonal antibody against GFP (1:1000; Abcam, AB13970); mouse monoclonal antibody against the embryonic form of myosin heavy chain MF20 (1:10; Developmental Studies Hybridoma Bank); and rabbit polyclonal antibody against RFP (1:1000; Abcam, AB62341). Species/isotype-specific secondary antibodies coupled with Alexa Fluor 488, 555 or 647 (Interchim) were used at 1:500 dilution.

Whole-mount embryos were examined using a Leica SP5 confocal microscope. Images were analyzed using Imaris (Bitplane) and ImageJ (NIH). All quantifications were performed by evaluating each fiber within optical sections of three-dimensional confocal stacks.

Statistics

Statistical analyses were performed using GraphPad Prism software. Each quantification is the result of analyses on a minimum of six embryos. To test whether the numbers of nuclei per fiber in each embryo of a given experimental series were statistically different, an analysis of variance (ANOVA) non-parametric testing was applied. We tested embryos against each other in the study of fusion during normal embryonic development. This analysis showed that there was no significant difference among embryos within an experimental series ($P>0.05$; not shown). This demonstrates that the results we obtained are highly reproducible despite the variability in electroporation efficiency that is inherent to the technique. It also indicates that each fiber of a given experimental series can be considered as a separate measurement for statistical purposes.

Mann–Whitney non-parametric two-tail testing was applied to populations of fibers to determine P-values. Numbers of examined fibers for each time point are indicated in supplementary material Tables S1

and S2. To evaluate the dependence of fiber length on nuclei number (Fig. 3D), the Pearson product-moment correlation coefficient was calculated using R software (http://www.r-project.org/) to determine the linear correlation (r) between the two variables: a value at or near 0 indicates that there is no association, whereas a value between 0.5 (−0.5) and 1 (or −1) indicates an increasingly strong positive (or negative) correlation; the P-value indicates the strength of this association. In Fig. 3D, r and the P-value were calculated separately for DML and dorsal dermomyotome; since they were nearly identical, they were averaged to determine the combined r and P-value in the trunk.

Acknowledgements
We thank Monash Micro Imaging (MMI) for imaging support; and Drs C. Hirst, N. Rosenthal and P. Currie for critical reading of the manuscript.

Competing interests
The authors declare no competing financial interests.

Author contributions
D.S.-M., M.D.L.C., M.P. and C.M. planned the experiments. D.S.-M., M.D.L.C and M.P. performed and analyzed the experiments. D.S.-M. and C.M. wrote the manuscript.

Funding
This work was supported by a grant from the National Health and Medical Research Council (NHMRC) of Australia, and by the EU 6th Framework Programme Network of Excellence MYORES to C.M.

Supplementary material
Supplementary material available online at
http://dev.biologists.org/lookup/suppl/doi:10.1242/dev.114546/-/DC1

References
Bate, M. (1990). The embryonic development of larval muscles in Drosophila. *Development* **110**, 791-804.
Ben-Yair, R. and Kalcheim, C. (2005). Lineage analysis of the avian dermomyotome sheet reveals the existence of single cells with both dermal and muscle progenitor fates. *Development* **132**, 689-701.
Brunner, S., Furtbauer, E., Sauer, T., Kursa, M. and Wagner, E. (2002). Overcoming the nuclear barrier: cell cycle independent nonviral gene transfer with linear polyethylenimine or electroporation. *Mol. Ther.* **5**, 80-86.
Bruusgaard, J. C., Liestøl, K. and Gundersen, K. (2003). Number and spatial distribution of nuclei in the muscle fibers of normal mice studied in vivo. *J. Physiol.* **551**, 467-478.
Cavalier-Smith, T. (1978). Nuclear volume control by nucleoskeletal DNA, selection for cell volume and cell growth rate, and the solution of the DNA C-value paradox. *J. Cell Biol.* **34**, 247-278.
Chevallier, A., Kieny, M. and Mauger, A. (1976). The origin of the wing musculature of birds. *C R. Acad. Sci. Hebd. Seances Acad. Sci. D* **282**, 309-311.
Christ, B., Jacob, H. J. and Jacob, M. (1974). Über den Ursprung der Flügelmuskulatur. Experimentelle Untersuchungen mit Wachtel- und Hühnerembryonen. *Experientia* **30**, 1446-1449.
Delfini, M.-C., De La Celle, M., Gros, J., Serralbo, O., Marics, I., Seux, M., Scaal, M. and Marcelle, C. (2009). The timing of emergence of muscle progenitors is controlled by an FGF/ERK/SNAIL1 pathway. *Dev. Biol.* **333**, 229-237.
Denetclaw, W. F. and Ordahl, C. P. (2000). The growth of the dermomyotome and formation of early myotome lineages in thoracolumbar somites of chicken embryos. *Development* **127**, 893-905.
Doberstein, S. K., Fetter, R. D., Mehta, A. Y. and Goodman, C. S. (1997). Genetic analysis of myoblast fusion: blown fuse is required for progression beyond the prefusion complex. *J. Cell Biol.* **136**, 1249-1261.
Goldstein, S., Fordis, C. M. and Howard, B. H. (1989). Enhanced transfection efficiency and improved cell survival after electroporation of G2/M-synchronized cells and treatment with sodium butyrate. *Nucleic Acids Res.* **17**, 3959-3971.
Gros, J., Scaal, M. and Marcelle, C. (2004). A two-step mechanism for myotome formation in chick. *Dev. Cell* **6**, 875-882.
Gros, J., Manceau, M., Thomé, V. and Marcelle, C. (2005). A common somitic origin for embryonic muscle progenitors and satellite cells. *Nature* **435**, 954-958.
Horsley, V., Friday, B. B., Matteson, S., Kegley, K. M., Gephart, J. and Pavlath, G. K. (2001). Regulation of the growth of multinucleated muscle cells by an NFATC2-dependent pathway. *J. Cell Biol.* **153**, 329-338.
Horsley, V., Jansen, K. M., Mills, S. T. and Pavlath, G. K. (2003). IL-4 acts as a myoblast recruitment factor during mammalian muscle growth. *Cell* **113**, 483-494.
Kahane, N., Cinnamon, Y. and Kalcheim, C. (2002). The roles of cell migration and myofiber intercalation in patterning formation of the postmitotic myotome. *Development* **129**, 2675-2687.
Kassar-Duchossoy, L., Giacone, E., Gayraud-Morel, B., Jory, A., Gomès, D. and Tajbakhsh, S. (2005). Pax3/Pax7 mark a novel population of primitive myogenic cells during development. *Genes Dev.* **19**, 1426-1431.
Knudsen, K. A. and Horwitz, A. F. (1977). Tandem events in myoblast fusion. *Dev. Biol.* **58**, 328-338.
Manceau, M., Gros, J., Savage, K., Thomé, V., McPherron, A., Paterson, B. and Marcelle, C. (2008). Myostatin promotes the terminal differentiation of embryonic muscle progenitors. *Genes Dev.* **22**, 668-681.
Moore, C. A., Parkin, C. A., Bidet, Y. and Ingham, P. W. (2007). A role for the Myoblast city homologues Dock1 and Dock5 and the adaptor proteins Crk and Crk-like in zebrafish myoblast fusion. *Development* **134**, 3145-3153.
Ordahl, C. P., Berdougo, E., Venters, S. J. and Denetclaw, W. F. J. (2001). The dermomyotome dorsomedial lip drives growth and morphogenesis of both the primary myotome and dermomyotome epithelium. *Development* **128**, 1731-1744.
Primmett, D. R., Stern, C. D. and Keynes, R. J. (1988). Heat shock causes repeated segmental anomalies in the chick embryo. *Development* **104**, 331-339.
Rash, J. E. and Fambrough, D. (1973). Ultrastructural and electrophysiological correlates of cell coupling and cytoplasmic fusion during myogenesis in vitro. *Dev. Biol.* **30**, 166-186.
Relaix, F., Rocancourt, D., Mansouri, A. and Buckingham, M. (2005). A Pax3/Pax7-dependent population of skeletal muscle progenitor cells. *Nature* **435**, 948-953.
Richardson, B. E., Nowak, S. J. and Baylies, M. K. (2008). Myoblast fusion in fly and vertebrates: new genes, new processes and new perspectives. *Traffic* **9**, 1050-1059.
Rios, A. C., Serralbo, O., Salgado, D. and Marcelle, C. (2011). Neural crest regulates myogenesis through the transient activation of NOTCH. *Nature* **473**, 532-535.
Rochlin, K., Yu, S., Roy, S. and Baylies, M. K. (2010). Myoblast fusion: when it takes more to make one. *Dev. Biol.* **341**, 66-83.
Scaal, M., Gros, J., Lesbros, C. and Marcelle, C. (2004). In ovo electroporation of avian somites. *Dev. Dyn.* **229**, 643-650.
Schienda, J., Engleka, K. A., Jun, S., Hansen, M. S., Epstein, J. A., Tabin, C. J., Kunkel, L. M. and Kardon, G. (2006). Somitic origin of limb muscle satellite and side population cells. *Proc. Natl. Acad. Sci. USA* **103**, 945-950.
Shavlakadze, T. and Grounds, M. (2006). Of bears, frogs, meat, mice and men: complexity of factors affecting skeletal muscle mass and fat. *Bioessays* **28**, 994-1009.
Simionescu, A. and Pavlath, G. K. (2011). Molecular mechanisms of myoblast fusion across species. *Adv. Exp. Med. Biol.* **713**, 113-135.
Srinivas, B. P., Woo, J., Leong, W. Y. and Roy, S. (2007). A conserved molecular pathway mediates myoblast fusion in insects and vertebrates. *Nat. Genet.* **39**, 781-786.
Venters, S. J., Hultner, M. L. and Ordahl, C. P. (2008). Somite cell cycle analysis using somite-staging to measure intrinsic developmental time. *Dev. Dyn.* **237**, 377-392.
Wakelam, M. J. (1985). The fusion of myoblasts. *Biochem. J.* **228**, 1-12.
White, R., Biérinx, A.-S., Gnocchi, V. and Zammit, P. (2010). Dynamics of muscle fibre growth during postnatal mouse development. *BMC Dev. Biol.* **10**, 21.

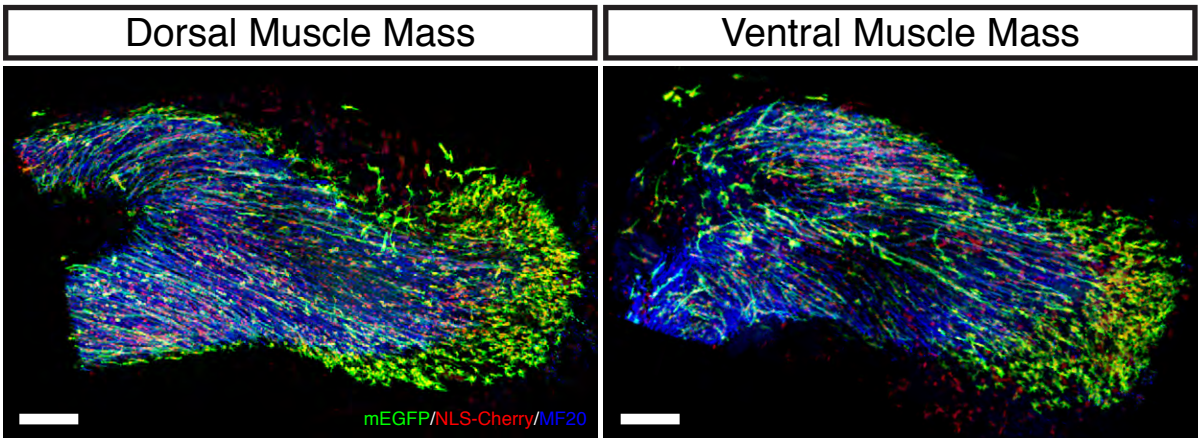

Supplementary Figure 1.

Dorsal and ventral muscle masses of a single E5.5 chick embryo forelimb co-electroporated at E2.5 in the VLL of somites in the forelimb region with EGFP (in green) and a nuclear form of mCherry (in red). In blue, immuno-staining against MyHC. This shows that the distribution of plurinucleated myofibers is similar in both muscle masses (longest fibers in the central domain, shortest at the periphery), while a cloud of mononucleated progenitors is present at the distal leading edge of both muscle masses.

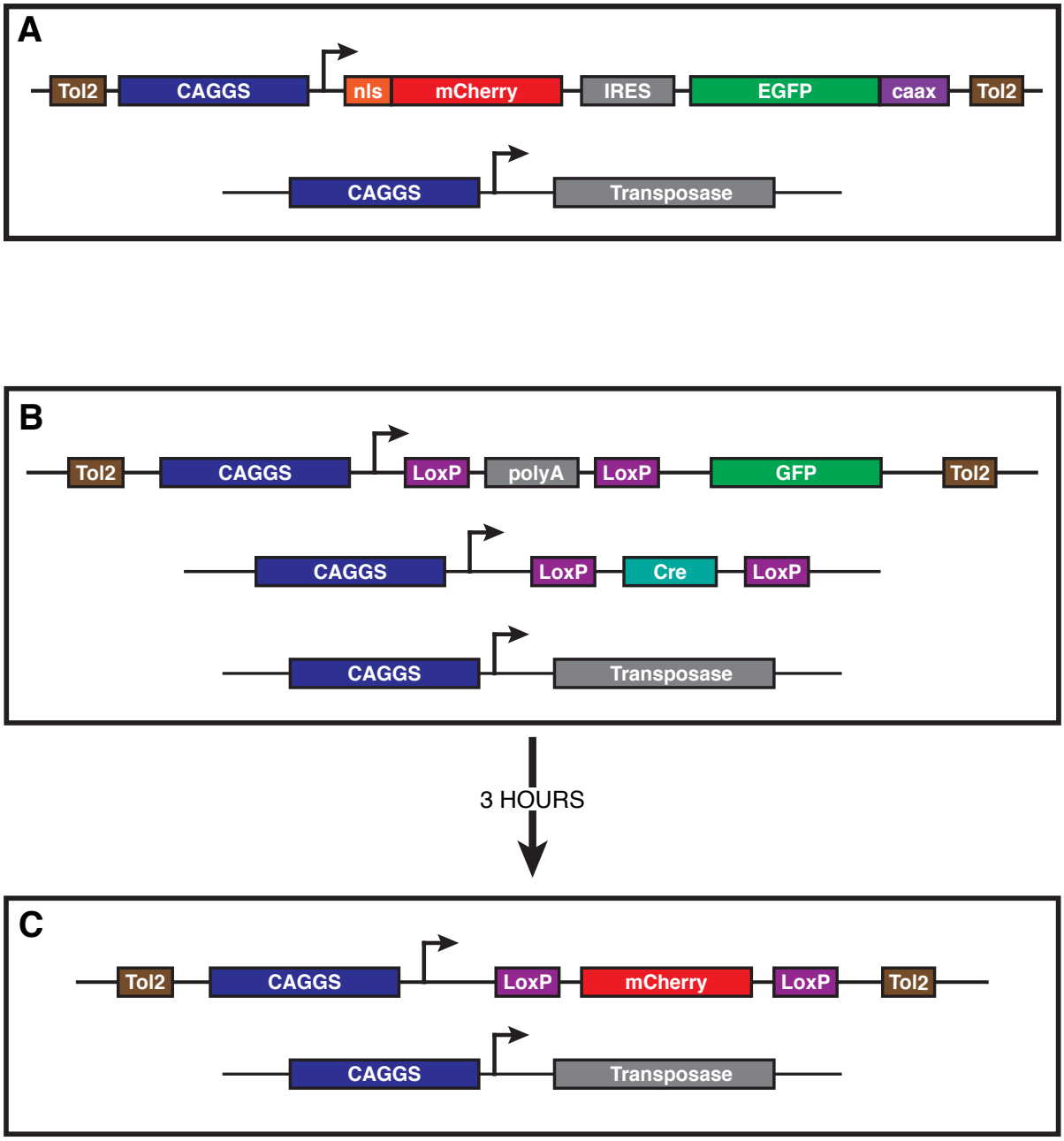

Supplementary Figure 2.

(A): Vectors utilized to count the number of nuclei per fiber. (B,C): Description of the double-electroporation protocol aimed at mosaically labelling a cell population with two fluorochromes. B: First co-electroporation with two plasmids, that encode a self-excising Cre and GFP, downstream of a floxed poly(A) signal. When both plasmids are co-expressed, epithelial cells are GFP-positive. If only one plasmid is expressed, cells are not fluorescent. (C): 4 hours later, the DML is electroporated once more with a plasmid encoding a floxed mCherry. DML cells express the mCherry fluorochrome, unless they were previously electroporated with Cre, which inactivates mCherry. The self-excising Cre ensures that the Cre protein is only temporarily present; if mosaically-labeled cells do not fuse, myocytes will be either red or green, if they fuse, a proportion of them will be yellow.

Supplementary Table 1.
Count of nuclei per fiber observed at the indicated times after DML, dorsal dermomyotome and limb electroporation.

	E3.5	E4	E4.5	E5	E5.5	E6
DML EP						
	n=189		n=353		n=336	
1N	176		265		68	
2N	12		75		98	
3N	1		10		80	
4N			3		44	
5N					33	
6N					11	
7N					2	
Mean	1.1		1.3		2.8	
Dm EP						
			n=186		n=223	
1N			80		40	
2N			71		54	
3N			24		58	
4N			10		41	
5N			1		21	
6N					7	
7N					1	
8N					1	
Mean			1.8		2.9	
LIMB EP						
		n=115	n=59	n=207	n=238	n=128
1N		103	47	37	4	6
2N		9	11	50	21	7
3N		3	1	30	24	9
4N				32	31	15
5N				15	25	15
6N				15	36	14
7N				11	25	12
8N				4	18	9
9N				5	21	7
10N				3	12	7
11N				1	8	12
12N					2	12
13N					1	2
14N						1
15N					1	1
16N				1	1	
17N						1
Mean		1.1	1.2	3.6	6.1	6.7

Supplementary Table 2.

GFP (green), mCherry (red) and mixed (yellow) fibers after electroporation of the indicated somite sub-populations.

DML/DML 10hpe no Cre				
		Green	**Red**	**Yellow**
	Fibers Counted	48	26	101
	Percentage Mean	26.7	14.7	58.6
	Standard Deviation	8.1	6.3	13.0
DML/DML 10hpe control				
		Green	**Red**	**Yellow**
	Fibers Counted	226	215	24
	Percentage Mean	46.9	49.7	3.4
	Standard Deviation	18.2	18.8	4.7
DML/DML 72hpe				
		Green	**Red**	**Yellow**
	Fibers Counted	193	150	49
	Percentage Mean (Adj.)	49.7	42.2	8.2
	Standard Deviation	7.6	13.2	6.6
Dm/Dm 72hpe				
		Green	**Red**	**Yellow**
	Fibers Counted	83	69	88
	Percentage Mean (Adj.)	36.7	30.2	33.1
	Standard Deviation	4.6	7.3	6.4
DML/Dm 72hpe				
		Green	**Red**	**Yellow**
	Fibers Counted	91	77	28
	Percentage Mean (Adj.)	48.0	42.7	9.3
	Standard Deviation	8.1	8.2	11.2
DML/AL 72hpe				
		Green	**Red**	**Yellow**
	Fibers Counted	78	66	42
	Percentage Mean (Adj.)	43.3	36.6	20.1
	Standard Deviation	11.3	8.8	7.8
DML/PL 72hpe				
		Green	**Red**	**Yellow**
	Fibers Counted	78	64	38
	Percentage Mean (Adj.)	45.1	37.1	17.8
	Standard Deviation	5.4	5.5	5.1